PAPER • OPEN ACCESS

Cyclic voltammetry studies of bioanode microbial fuel fells from batch culture of *Geobacter sulfurreducens*

To cite this article: N F Shoparwe *et al* 2021 *IOP Conf. Ser.: Earth Environ. Sci.* **765** 012102

View the article online for updates and enhancements.

Cyclic voltammetry studies of bioanode microbial fuel fells from batch culture of *Geobacter sulfurreducens*

N F Shoparwe[1,*], M M Z Makhtar[2], S A Sata[3], W S Kew[1], M Mohamad[1] and H Shukor[4]

[1]Faculty of Bioengineering and Technology, Jeli Campus, Universiti Malaysia Kelantan, 17600 Jeli Kelantan, Malaysia
[2]Bioprocess Technology Division, School of Industrial Technology, Universiti Sains Malaysia, 11800 Pulau Pinang, Malaysia
[3]School of Chemical Engineering, Universiti Sains Malaysia, 14300 Nibong Tebal, Pulau Pinang, Malaysia
[4]Centre of Excellence Biomass Utilization, Faculty of Chemical Engineering Technology, Universiti Malaysia Perlis, 02600 Arau Perlis, Malaysia

*E-mail: fazliani.s@umk.edu.my

Abstract. The present study aims to investigate the performance of batch culture of *Geobacter sulfurreducens (G. sulfurreducens)* for electrical current generation via cyclic voltammetry (CV) method. The CV study was performed with an applied voltage in the range of -0.1 to 0.1 V against the standard calomel electrode (SCE) during the cell growth and attachment of *G. sulfurreducens* on graphite felt and initial acetate concentration of 20 mM. The kinetics of electrode reaction was investigated by conducting CV experiments at different scanning rates of 5, 10, 20, 50 and 100 mVs^{-1}. The diffusion coefficients (D) and heterogeneous electron transfer rate constant (k_o) of both anodic and cathodic process were 1.04 x10^{-5} cm^2.s^{-1}, 1.73x10^{-6} cm^2.s^{-1}, 0.0004 cm.s^{-1} and 0.0011 cm.s^{-1}, respectively. The obtained results showed that the anode exhibits high bioeletrocatalytic activity due to the attachment of *G. sulfurreducens* on the anode surface.

1. Introduction

Cyclic voltammetry (CV) is the most widely used technique for acquiring qualitative and quantitative information on electrochemical reactions [1]. Currently, the use of CV method seems to be increasing tremendously in popularity and is becoming an essential method in microbial fuel cells research. The three main purpose for applying CV method in microbial fuel cell studies includes: (i) to determine the redox potential of species involved at different operating conditions [2-11], (ii) to characterize the mechanism of electron transfer between the biocatalyst and bioanode or biocathode [7, 12-15], and (iii) to interpret the anodic electron transfer at different stages of microbial growth and metabolic activity [1, 16-23]. Although, much research has been conducted via applying CV's method in microbial fuel cells. However, most of the works reported did not give further analysis on important parameters in CV methods including heterogeneous electron transfer rate (k_o) and diffusion coefficient (D). These parameters are crucial in order to present the electron transfer performance in microbial fuel cells. Therefore, in this paper, a detailed CV study of anode microbial fuel cells during *G. sulfurreducens* growth, attachment on graphite felt and electric current generation as function of time were performed.

The CV experiment was conducted at different scanning rate and voltage was changed from -1.0 V to 1.0 V against the reference electrode of standard calomel electrode (SCE). In order to obtain the peak separation of the redox process of each cyclic voltammograms, the reversibility study and electrode kinetic were performed based on Randles Sevcik equation [24] and Nicholson and Shain Nicholson and Shain [25] theory. Two of the most commonly used evaluation criteria, (D) and (k_o) that represents CV performance were also determined in this study.

2. Methodology

2.1. Microorganism and culture conditions

The bacteria, *G. sulfurreducens* strain PCA (ATCC 51573) was obtained from the American Type Culture Collection (ATCC, Rockville, MD). The strain was subcultured in the laboratory at 30 ℃ and incubated under anaerobic condition. The growth medium was prepared according to the protocol supplied by ATCC which consists of the following: 1.5 g/L of NH_4Cl, 0.6 g/L of NaH_2PO_4, 0.1 g/L of KCl, 2.5 g/L of $NaHCO_3$, 50 ml/L Wolfe's vitamin mix solution and 10.0 ml/L modified Wolfe's mix mineral solution. The medium was added with 50 mM sodium fumarate as electron acceptor and 20 mM sodium acetate as electron donor [14].

2.2. Bioelectrochemical Set-up and CV analysis

Bioelectrochemical experiment was conducted using a fabricated single glass as shown in Figure 1. A proton exchange membrane (PEM) (Nafion 117, DuPont Co., USA) was used to separate the anode and cathode compartments thereby allowing the transfer of H^+ ions through the membrane. The anode was a graphite felt (Morgan AM&T, Greenville USA), and the cathode was a graphite plate, both having a dimension of 25.0 cm^2 each. The working volume of the anode component was 500 cm^3. The assembled microbial fuel cells were autoclaved at 121 ℃ for 20 min. A SCE (+0.242 V versus standard hydrogen electrode, SHE) (ALS Co., Ltd, Tokyo, JAPAN) was used as a reference electrode (RE). The CV experiments were conducted using three electrode setup.
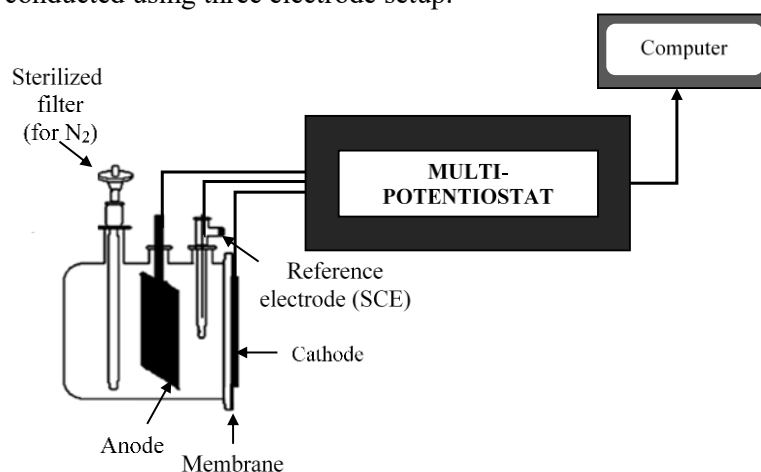
Figure 1. Schematic diagram of the single-chamber microbial fuel cell connected to multi-potentiostat and computer.

2.3. CV experiment and Analysis

In this experiment, each of the microbial fuel cell was connected to the multi-potentiostat (VMP3 Biologic SA) using three-electrode set-up. The CV profile was analysized using (software EC-Lab®, version 10. 3, Bio-Logic S.A.S). Reversibility test of cyclic voltammogram were analyzed based on Pletcher et al. [24]. The diffusion coefficient of anode and cathode for the system was determined using quasi-reversible Randles-Servcik equation as represented in equation (1) [24]:

$$I_P = \pm(2.65 \times 10^5)\alpha n^{1/2} ACD^{1/2} \upsilon^{1/2} \tag{1}$$

where I_p is the peak of electric current (mA), D is the diffusion coefficient (cm^2.s^{-1}), υ is the potential scan rate (V.s^{-1}), n is the number of electron, α is the transfer coefficient, A is the electrode surface area and C is the concentration of species in bulk solution (mol/cm^3). The non-linear least-squares regression of Lavenberg-Maquadrt method using Polymath@ Version 6.10 (CACHE Corpn, USA) was employed in order to estimate the value of parameters within the non-linear model [26]. The parameters obtained from peaks of CV were used to determine the heterogeneous electron transfer rate constant (k_o). The k_o value was determined from the equation proposed by Nicholson and Shain [25] as represented in equation (2) and (3):

$$E_P = K - \frac{2.3RT}{2\alpha nF} \log(\upsilon) \tag{2}$$

where,

$$K = E_e^\circ - \frac{RT}{\alpha nF}\left(0.78 - \frac{2.3}{2}\log\left(\frac{\alpha nFD}{k_o^2 RT}\right)\right) \tag{3}$$

where E_e° is the formal standard potential, E_P is the peak potential either for anode or cathode, α is the charge transfer coefficient, n is number of the electrons transferred during the oxidation, F is Faraday constant (96,485 C.mol^{-1}), k_o is the standard heterogeneous rate constant, υ is the potential scan rate (V.s^{-1}), T is the temperature and R is the gas constant (8.314 J.K^{-1}.mol^{-1}). The peak of the anodic and cathodic potential against log scanning rate of the cyclic voltammogram was plotted and a linear relationship of this plot resulted in a slope (m) and intercept (y) for the value of *K*. By substituting the values of slope and intercept (y) obtained from the linear relationship, the value of αn was obtained. The value of heterogeneous electron transfer (k_o) could be determined by rearranging equation (2) and substituting the value of αn and other parameter values in equation (3).

2.4 Reversibility test of cyclic voltammogram
The main peak of anode and cathode for CV's experiment were analyzed using a polynomial baseline method as described in the manual of EC-Lab Software. The diagnostic tests for reversible, quasi-reversible and irreversible characteristic were then determined by plotting peak current (I_P) as a function of the square root of scan rate ($v^{1/2}$). The results were compared with Figure 2, which illustrates the electrochemical behaviors that depends on the applied voltammetric scanning rate. Further diagnostic tests for reversibility characteristic as described by Pletcher et al. [24] were also applied.
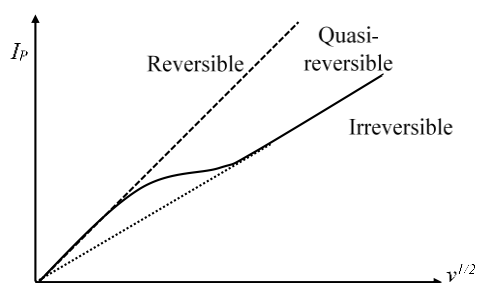

Figure 2. A plot of the peak electric current (I_p) corresponding to the square root of the potential sweep (scanning) rate, showing the behaviours of the reversible, quasi-reversible and irreversible phases [24].

3. Results and Discussion

### *3.1   The general characteristics of CV response*

The general characteristics of CV using different plots of responses for an anode microbial fuel cell are shown in Figure 2 (a)-(c). The figure shows one of the voltage sweep and electric current response for an experiment using graphite felt as an anode. Figure 2(a) shows the potential waveform as a function of time which was recorded with a scan rate of 100 mV/s and potential sweep from -1.0 V to 1.0 V. During the scan, the flowing electric current with time was recorded and shown in Figure 3 (b). The electric current tends to increase as it reaches the oxidation potential of the electroactive species but drops when the electroactive species was consumed or reacts close to the electrode surface. Figure 3 (c) shows the electric current as a function of the potential, known as a cyclic voltammogram [1]. This figure depicts one of the CV responses for the oxidation and reduction of an anode microbial fuel cell. As seen from the shape of this cyclic voltammogram, the potential was scanned in the positive direction (oxidation), whereby the electric current rose to a peak and decayed in a regular manner. Theoretically, the production of electric current depends on two steps in the overall process; (i) the movement of electroactive species to the surface, and (ii) the electron transfer reaction [4]. There were two oxidation peaks (peak 1 and peak 2) during the anodic scan and two reduction peaks (peak 3 and peak 4) formed, as presented in Figure 3 (c). The first oxidation peak (peak 1) and second oxidation peak (peak 2) during the anode scan were observed at about 0.491 V and -0.662, respectively. These peaks were accompanied by the appearance of two reduction peaks during the reverse scan at about 0.127 V and -0.706 V for peak 3 and peak 4, respectively. These oxidation and reduction peaks were observed in a large potential region, revealing the existence of four distinct redox couples. These redox couples suggest that the different redox species in the bacteria contributes to the intensities of the electric current.
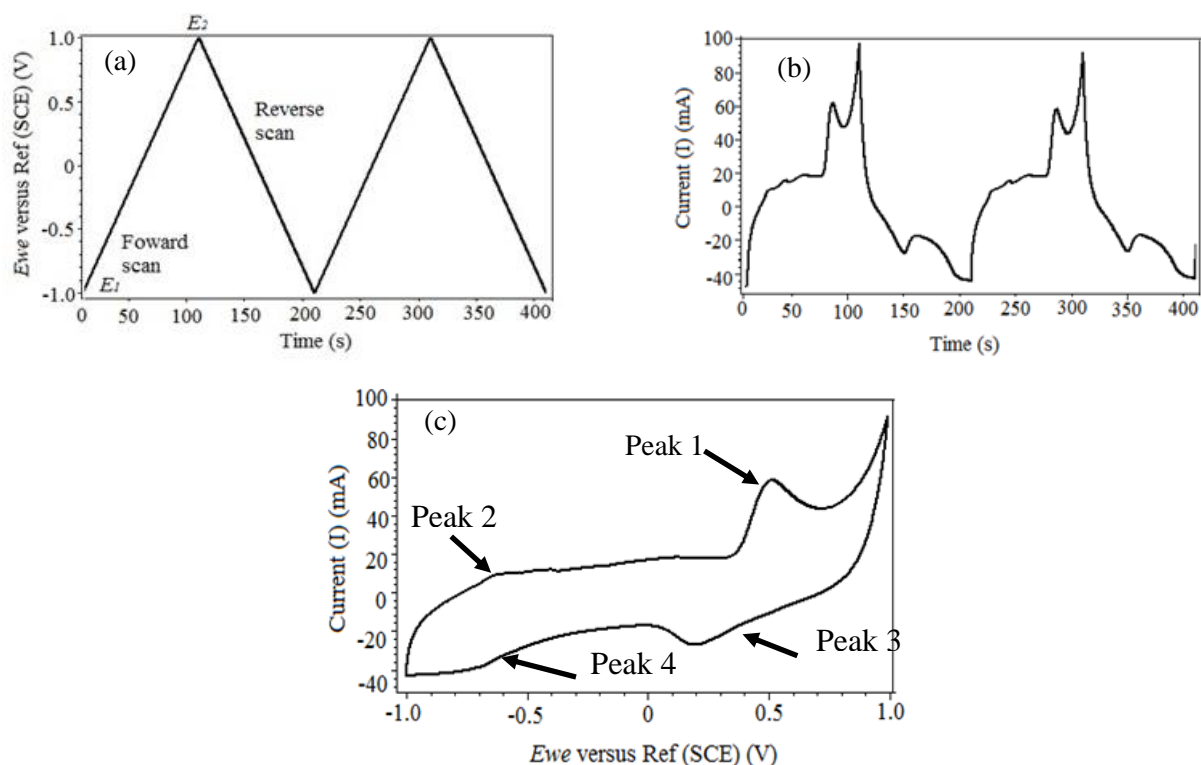

Figure 3.(a). Potential waveform, (b). electric current vs time, and (c). electric current vs potential of CV experiment in microbial fuel cell system.

3.2   CV studies during the cell growth and biofilm formation in a batch system

The results of cyclic voltammograms exhibiting different behaviours depending on the growth stage of *G. sulfurreducens* are shown in Figure 4. The cyclic voltammograms against fermentation time are presented in Figure 5. CV parameters including the anodic peak potential (E_{PA}), cathodic peak potential (E_{PC}), anodic peak electric current (I_{PA}), cathodic peak electric current (I_{PC}), the shape factor (E_P-$E_{P/2}$), positive charge and negative charge were determined from each cyclic voltammogram. The total values of these parameters for each peak (peak 1, peak 2, peak 3 and peak 4) are presented in Table 1. Prior to inoculation, the cyclic voltammograms did not show any redox peak during the oxidation and reduction process (Figure 5 (a)). After 48 hours of inoculation, multiple redox peaks began to appear across the potential window scan (Figure 5 (b)). Then, after 72 hours of incubation (Figure 5 (c)), the oxidation and reduction peaks began to increase and finally reached its maximum value after 96 hours (Figure 5 (d)). The value of positive charge was also higher in this condition (Table 1). These observations are parallel with the cell growth and electric current profile as shown in Figure 4. The cell growth increased over a couple of days and reached its maximum value after 72 hours of fermentation time and reached the exponential phase. The increasing electric current based on these oxidation and reduction peaks might be due to several reasons. According to Logan [27], when microorganisms interact with conductive solid surface (electrode), they will start to attach to the surface and form electroactive microbial biofilms. The cells on the anode surface are able to produce an electron shuttle compound (an oxidized and reduced redox protein) to transfer the electrons for electric current generation [28]. In the case of the *G. sulfurreducens* cells, numerous studies claimed that c-type cytochromes located on the microbes outer membrane are the key redox species that participate in extracellular electron transfer [12, 18, 29-33].The measured redox potentials as indicated by the CV results were compared to redox peaks reported by Esteve-Núñez et al. [34] and Zhu et al. [35]. Accordingly, the result proves that the electron transport system for the *G. sulfurreducens* cells consist of various types of cytochromes assisting the electron transfer in anode microbial fuel cells. The results of the cyclic voltammogram obtained in this study are also in agreement with previous studies regarding the availability of different c-cytochromes groups in *G. sulfurreducens* cells which can be oxidized at different potentials [12, 36, 37]. Moreover, the increasing oxidation and reduction peaks may be due to the increasing redox ratio of the reduced and oxidized protein, which can result to a dramatic increase in the electric current [5]. The oxidized and reduced redox compound were presumably produced in a significant amount after bacterial enrichment. This period of enrichment can be ascribed to substrate availability and biofilm formations, which had been proven by previous studies [38, 39]. A mature biofilm on the anode was also necessary for a stable and higher electric current generation [22, 40].
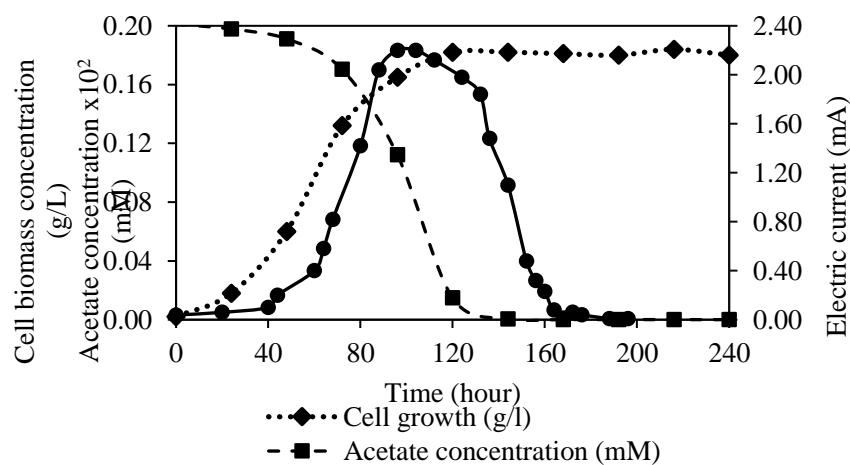
Figure 4. Growth profile of *G. sulfurreducens*, acetate utilization and electrical current production.
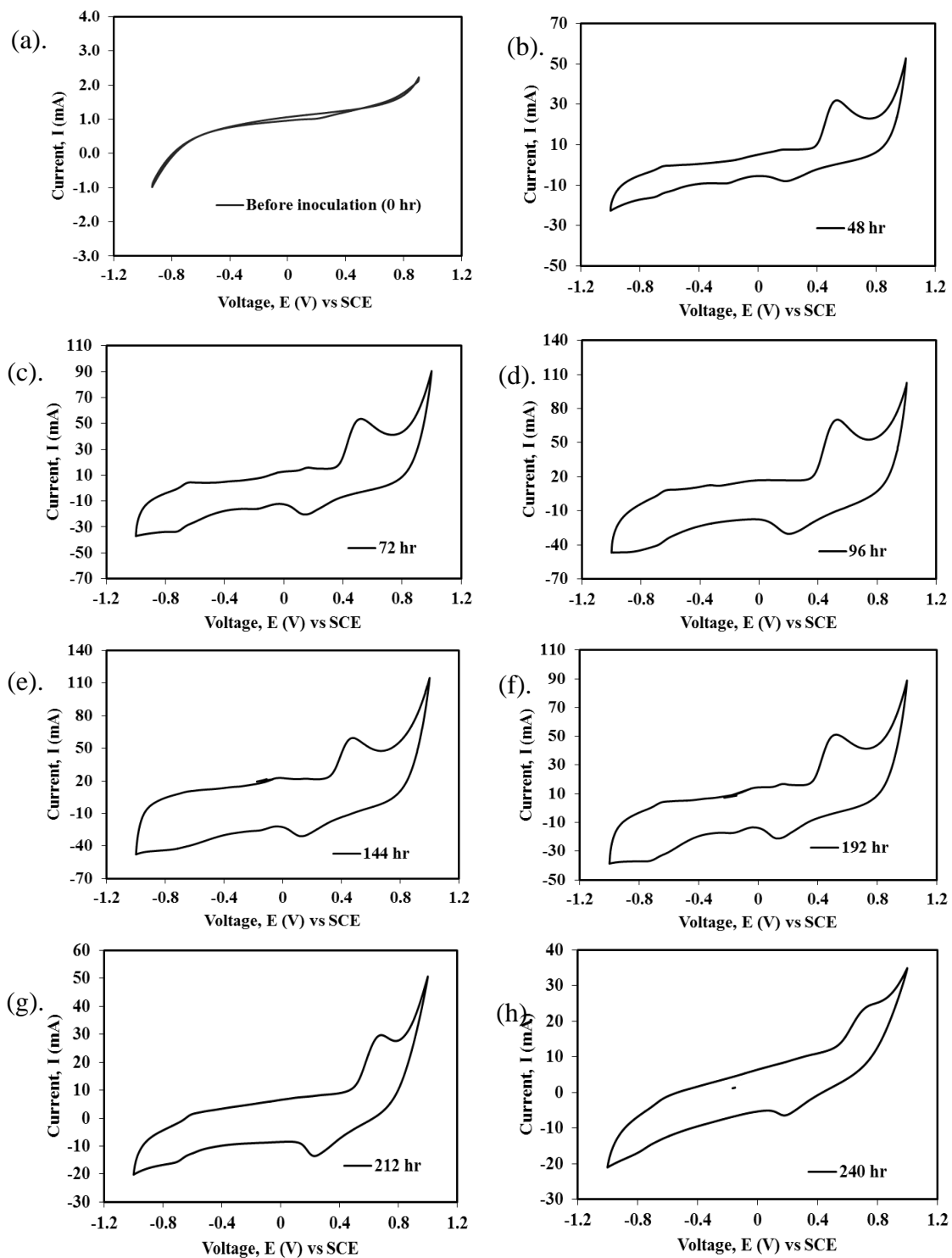
Figure 5. Typical cyclic voltammogram recorded at 100 mVs^{-1} and potential sweeps from -1.0 to 1.0 V of batch culture of the *G. sulfurreducens* in an anode microbial fuel cells (20 mM initial acetate concentration) for (a). 0, (b). 48, (c). 72, (d). 96, (e). 144, (f). 192, (g) 212, and (h). 240 hour (Batch system: initial substrate concentration=20 mM).
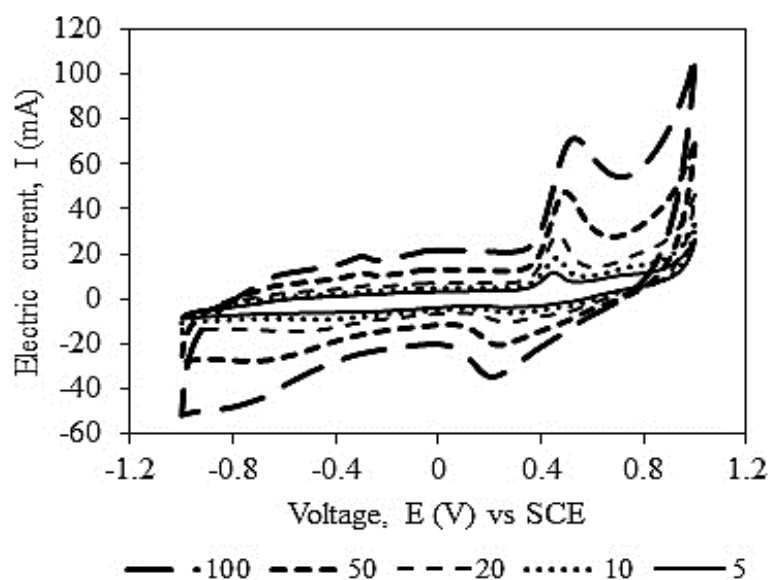
Table 1. Parameters of cyclic voltammogram

Peak Time	Parameters	Oxidation peak		Reduction peak	
		Peak 1	Peak 2	Peak 4	Peak 5
0 hour		No oxidation and reduction peak			
48 hours	E_p (V)	0.558	-0.634	0.169	-0.708
	Ip (mA)	19.35	6.554	7.726	2.704
	E_p-$E_{p/2}$ (V)	0.065	0.107	0.144	0.054
	Charge (+) (mC)	41.52	19.00	0	0.486
	Charge (-) (mC)	-33.54×10^{-6}	0	-20.47	-3.55
72 hours	E_p (V)	0.506	-0.652	0.147	-0.727
	Ip (mA)	32.12	10.09	12.04	6.58
	E_p-$E_{p/2}$ (V)	0.078	0.248	0.139	0.115
	Charge (+) (mC)	61.73	33.65	58.7×10^{-6}	2.25×10^{-3}
	Charge (-) (mC)	-0.144	0	-28.43	-14.83
96 hours	E_p (V)	0.491	-0.662	0.127	-0.706
	Ip (mA)	39.46	14.93	17.42	9.99
	E_p-$E_{p/2}$ (V)	0.088	0.264	0.253	0.319
	Charge (+) (mC)	86.46	65.26	0	2.32×10^{-3}
	Charge (-) (mC)	-20.97×10^{-6}	0	-57.68	-32.18
144 hours	E_p (V)	0.464	-0.671	0.145	-0.721
	Ip (mA)	30.34	7.87	12.18	3.16
	E_p-$E_{p/2}$ (V)	0.075	0.215	0.143	0.184
	Charge (+) (mC)	55.30	33.73	0	0.124
	Charge (-) (mC)	-0.26	0	-30.45	-9.08
192 hours	E_p (V)	0.501	-0.649	0.141	-0.718
	Ip (mA)	24.13	6.795	10.90	6.725
	E_p-$E_{p/2}$ (V)	0.075	0.227	0.137	0.157
	Charge (+) (mC)	48.29	34.67	0	0
	Charge (-) (mC)	-0.022	-0.731	-25.25	-18.78
212 hours	E_p (V)	0.563	-0.596	0.230	-0.696
	Ip (mA)	11.19	3.14	6.69	0.45
	E_p-$E_{p/2}$ (V)	0.081	0.252	0.134	0.091
	Charge (+) (mC)	19.72	11.57	0	0.47
	Charge (-) (mC)	-0.011	0	-15.49	-0.411
240 hours	E_p (V)	0.606	-0.533	0.198	-0.712
	Ip (mA)	3.13	1.58	3.24	0.22
	E_p-$E_{p/2}$ (V)	0.079	0.306	0.122	0.048
	Charge (+) (mC)	5.01	5.09	0	0.386
	Charge (-) (mC)	-15.12×10^{-6}	0	-6.05	-0.227

3.3   CV studies at different scanning rate and reversibility studies
To understand the oxidation and reduction characteristic of anode microbial fuel cells, CV's experiment was recorded at varying scan rates (5, 10, 20, 50 and 100 mV.s^{-1}). Cyclic voltammograms were recorded and represented in Figure 6. The results showed that, with increase in scan rate, both peak of anode and cathode electric current increases and the cathodic potential shifted towards a negative value, while anodic peak potential move towards a more positive value. The cyclic voltammograms were analyzed using EC Lab software to identify the peak of anodic and cathodic electric currents and potential. In this study, the only main peak of oxidation and reduction were analyzed which can be assumed as the only

simple electrode reaction involved in the system. The results obtained from the software for each cyclic voltammogram are presented in Table 2. The peak of electric current (I_P) obtained at different square root of scan rate for oxidation and reduction peak were plotted and represented in Figure 6 (a) and (b). Figure 6 (a) and (b) were compared with Figure 2 in order to characterize the reversibility behaviour of cyclic voltammogram. It was found that at scanning rates of 5, 10, and 20 mVs^{-1}, the electrochemical equilibrium (reversible process) was maintained on the electrode surface. A linear relationship between the peak of electrical current and the square root of the scan rate indicates that the behaviour undergoes a diffusion-controlled process. The linear relationship from the plotted data points can be characterized using the Randles-Servičk equation for a reversible process [24]. This linear relationship did not start from the origin due to the non-faradic electrical current which signifies that no chemical reactions (charge transfer) was involved at the beginning of the process. This will lead to the accumulation and removal of electrical charges on the electrode as well as the electrolyte solution near the electrode known as the electrochemical double layer [41]. However, at a higher scanning rate (above 50 mVs^{-1}), the linear portion deviates from following the Randles-Servičk plot, producing a non-linear curve which is in relationship with the quasi-reversible as shown in Figure 2. The observed deviation from higher scanning rate shown in Figure 7 (a) and (b) signifies that an insufficient electroactive species tends to move from solution to the electrode. Larger peak separations above 220 mV at higher scan rates could also be associated with a slow electron transfer or changes in the composition of the passive layer. At this condition, diffusion is not particularly efficient while mass transport and kinetic control dominates the process [24]. In order to confirm the reversibility status of the process, the data of peak analysis shown in Table 2 were evaluated. The ratio of the peak of oxidation electric current to its corresponding reduction counterpart, I_{pa}/I_{pc} is about 1.95 to 2.79. The peak ratio decreased with increase in scanning rate. In addition, the peak potential separation $\Delta E_P = E_{pa} - E_{pc}$ was between 60 to 306 mV. This value increased upon varying the scanning rate. The results obtained in Figure 7 (a)-(b) and Table 2 is an evidence that the redox process followed a quasi-reversible reaction rather than reversible reaction or irreversible reaction.

Figure 6. Cyclic voltammogram at different scanning rate.

Table 2. Parameters obtained from cyclic voltammogram at different scanning rate

Parameter	Scan Rate				
	100	**50**	**20**	**10**	**5**
	Oxidation peak				
E_{pa} (V)	0.511	0.494	0.472	0.456	0.442
I_{pa} (mA)	33.43	27.59	17.46	10.23	5.621
Log I_{pa} (mA)	1.524	1.441	1.242	1.009	0.749
E_p-$E_{p/2}$ (V)	0.0732	0.0613	0.053	0.047	0.0468
Charge (+) (mC)	57.37	80.12	97.66	97.94	101.4
Charge (-) (mC)	-1.126	-0.101	-0.083	-0.0286	-0.0998
	Reduction peak				
E_{pc} (V)	0.212	0.269	0.331	0.362	0.389
I_{pc} (mA)	17.14	13.12	7.349	4.251	2.015
Log I_{pc} (mA)	1.234	1.118	0.867	0.628	0.304
E_{pc}-$E_{pc/2}$ (V)	0.264	0.291	0.319	0.236	0.191
Charge (+) (mC)	0	0	0	0	0
Charge (-) (mC)	-72.74	-108.9	-157.2	-126.9	-166.5
	Oxidation and reduction peak ratio				
E_{pa}-E_{pc} (V)	306	223	138	94	60
I_{pa}/I_{pc}	1.951	2.103	2.376	2.406	2.790
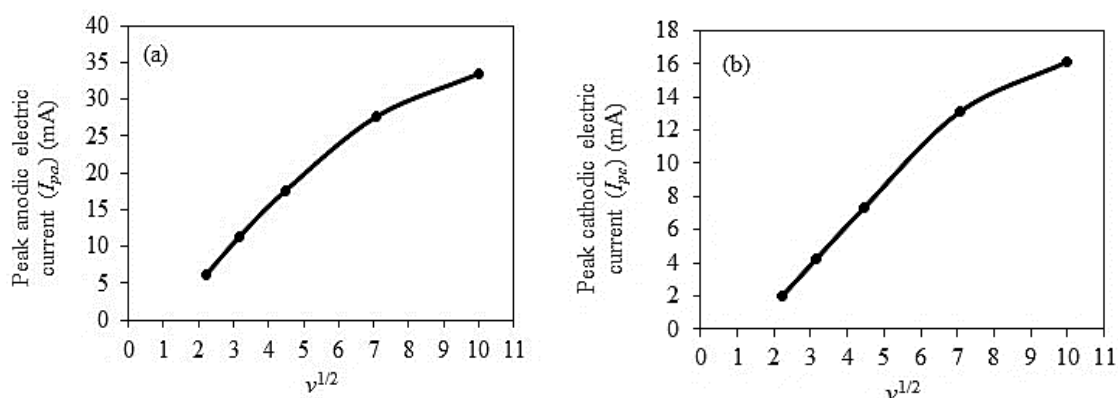
Figure 7. Plot of (a). anodic, and (b). cathodic of peak electric current (mA) versus square root of scan rate $(mV.s^{-1})^{1/2}$.

3.4   Diffusion coefficient (D) and heterogeneous electron transfer rate constant (k_o) of anode system
The peak characterization obtained from cyclic voltammogram can be used to determine the value of D and k_o. By substituting the I_p data at different $v^{1/2}$ (Figure 8) in equation (1) using the non-linear scheme in polymath software, the value of D for anodic and cathodic reaction was 1.04×10^{-5} cm^2.s^{-1} and 1.73×10^{-6} cm^2.s^{-1}, respectively. These two values slightly differ due to the difference in the state of complexation.

Based on equation (2) and (3), the value of k_o obtained for anodic and cathodic process were 0.0004 cm.s^{-1} and 0.0011 cm.s^{-1}, respectively. These value falls within the range of quasi-reversible conditions.
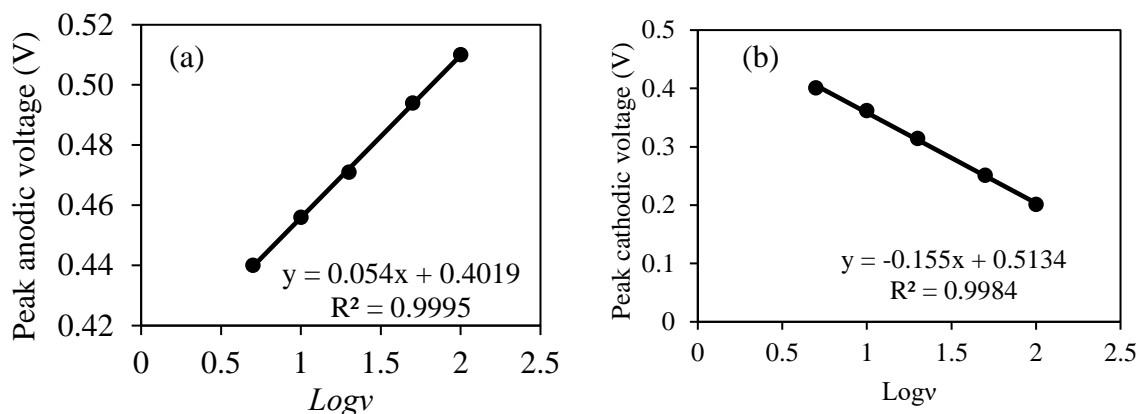
Figure 8. Plot of cathodic peak electric current (mA) versus square root of scan rate (mV/s)$^{1/2}$.

4. Conclusion

This paper presents the CV behaviour of *G. sulfureducens* culture in batch anode microbial fuel cells. The results show the significant change in CV results during the *G. sulfureducens* growth, attachment on graphite felt surface, acetate consumption and electrical current generation as a function of time. The kinetic of electrode reaction was performed using CV method at different scanning rates of 5, 10, 20, 50 and 100 mVs^{-1} and result revealed that the oxidation-reduction reaction in the batch anode microbial fuel cell system follows the quasi-reversible process. The value of D and k_o for anode process are 1.04 x10^{-5} cm^2.s^{-1} and 0.0004 cm.s^{-1}, whereas the cathodic process presents a value of 1.73x10^{-6} cm^2.s^{-1} and 0.0011 cm.s^{-1} for D and k_o, respectively.

References

[1]   Wang J (2006) *Analytical electrochemistry*, Vol. Third Edition ed., John Wiley & Sons
[2]   Rahimnejad M, Ghoreyshi A A, Najafpour G, and Jafary T 2011 *Applied Energy* **88** 3999-4004
[3]   Harnisch F and Freguia S 2012 *Chemistry–An Asian Journal* **7** 466-475
[4]   Tkach O, Liu L, and Wang A 2015) *J. Clean Energy Technol* **4** 36
[5]   Kim H J, Park H S, Hyun M S and Kim B H 2002 *Enzyme and Microbial Technology* **30**145-152
[6]   Chae K J, Choi M J, Lee J W, Kim K Y and Kim I S 2009 *Bioresource technology* **100** 3518-3525
[7]   Schröder U 2007 *Physical Chemistry Chemical Physics* **9** 2619-262
[8]   Wang X, Saito T and Logan B E 2009 *Environmental science & technology* **43** 6870-6874
[9]   Guo K, Keller J, and Rabaey K 2013 *Environmental science & technology* **47** 7563-7570
[10]   Anwer A, Khan M, and Khan M 2019 *Journal of environmental management* **249** 109376
[11]   Jackson M N, Pegis M L, and Surendranath Y 2019 *ACS central science* **5** 831-841.
[12]   Richter H, Lovley D R, and Tender L M 2009 *Energy and Environmental Science* **2** 506-516
[13]   Torres C I , Marcus A K R., and Rittmann B E 2010 *FEMS microbiology reviews* **34** 3-17
[14]   Shoparwe N F, M H Uzir, and S A Sata 2015 *Springer* 347-354
[15]   Chen G W, Lee T H, and Kim C W 2010 *Korean Journal of Chemical Engineering* **27** 1513-1520
[16]   Vielstich W 2010 *Cyclic voltammetry*, Wiley Online Library
[17]   Fricke K, Harnisch F and Schröder U 2008 *Energy & Environmental Science* **1** 144-147
[18]   Marsili E, Sun J, and Bond D R 2010 *Electroanalysis* **22** 865-874
[19]   Zhao Y, Li P, Wang X and Sun Y 2012 *Journal of Fuel Chemistry and Technology* **40** 967-972

[20]   Xie X, Hu L, Pasta M, Wells G F, Kong D, Criddle C S and Cui Y 2010 *Nano Letters* **11** 291-296

[21]   Liu T, Rao L, Yuan Y, and Zhuang L 2015 *The Scientific World Journal 2015*

[22]   Muaz M Z M, Abdul R and Vadivelu V M 2018 *Environmental Progress & Sustainable Energy* **38** 209-219

[23]   Jin X, Guo F, Liu Z, Liu Y and Liu H 2018 *Frontiers in Microbiology* **9** 2633.

[24]   Pletcher D, Greff R, Peat R, Peter L and Robinson J 2001 *Instrumental methods in electrochemistry*, Elsevier

[25]   Nicholson R S and Shain I 1964 *Analytical Chemistry* **36** 706-723.

[26]   Don M M and Shoparwe N F 2010 *Biochemical Engineering Journal* **49** 95-103.

[27]   Logan B E 2008 *Microbial fuel cells* John Wiley & Sons

[28]   Bond D R and Lovley D R 2003 *Applied and Environmental Microbiology* **69** 1548-1555.

[29]   Holmes D E, Chaudhuri S K, Nevin K P, Mehta T, Methé B A, Liu A, Ward J E, Woodar T L, Webster J, and Lovley D R 2006 *Environmental Microbiology* **8** 1805-1815

[30]   Lovley D R, Nevin K P, Holmes D E, Chauduri S, Mehta T and Methe B 2004 Mechanisms for electron transfer to electrodes in mediator-free microbial fuel cells, 2 ed.,1478-1480.

[31]   Esteve-Núñez A, Visconti P, and Lovley D R 2008 *Environmental Microbiology* **10** 497-505

[32]   Hernandez M, and Newman D 2001 *Cellular and Molecular Life Sciences* **58** 1562-1571

[33]   Methe B, Nelson K E, Eisen J, Paulsen I, Nelson W, Heidelberg J, Wu D, Wu M, Ward N and Beanan M 2003 *Science* **302** 1967-1969

[34]   Esteve-Núñez A, Busalmen J P, Berná A, Gutiérrez-Garrán C, and Feliu J M 2011 *Energy & Environmental Science* **4** 2066-2069

[35]   Zhu X, Yates M D, and Logan B E 2012 *Electrochemistry Communications* **22** 116-119

[36]   Mehta T, Coppi M V, Childers S E and Lovley D R 2005 *Applied and environmental microbiology* **71** 8634-8641

[37]   Strycharz S M, Glaven R H, Coppi M V, Gannon S M, Perpetua L A, Liu A, Nevin K P and Lovley D R 2011 *Bioelectrochemistry* **80** 142-150

[38]   Patil S A, Harnisch F, Koch C, Hübschmann T, Fetzer I, Carmona-Martínez A A, Müller S and Schröder U 2011 *Bioresource Technology* **102** 9683-9690

[39]   Muaz M Z M and Tajarudin H A 2020 International of Energy Research **44** 3260-3265

[40]   Zhang L, Zhu X, Li J, Liao Q and Ye D 2011 *Journal of Power Sources* **196** 6029-6035

[41]   Yu A, Chabot V and Zhang J 2013 *Electrochemical supercapacitors for energy storage and delivery: fundamentals and applications*, CRC Press.